PERGAMON

Deep-Sea Research I 48 (2001) 1553–1580

DEEP-SEA RESEARCH
PART I

www.elsevier.com/locate/dsr

Structure of the North Atlantic current in stream-coordinates and the circulation in the Newfoundland basin

C.S. Meinen*

Graduate School of Oceanography, University of Rhode Island, Narragansett, RI 02882, USA

Received 17 April 2000; received in revised form 27 June 2000; accepted 17 November 2000

Abstract

Accurate knowledge of the absolute North Atlantic Current (NAC) transport has been limited in the past by the difficulty of obtaining absolute velocity measurements. For this study, historical hydrography was combined with time series of round trip travel time from inverted echo sounders, bottom pressure sensor measurements, and measured velocities from deep current meters, via a "Gravest Empirical Mode" technique, to yield time series of temperature and absolute velocity sections. These sections were used to determine the mean NAC stream-coordinates structure of temperature and absolute velocity for the period from August 1993 to February 1995. This structure is narrower and stronger than the corresponding Eulerian average, with peak speeds greater than 80 cm s^{-1} and bottom velocities exceeding 10 cm s^{-1}. The calculated mean NAC transport was 131 ± 14 ($\times 10^6$ m^3 s^{-1}); temporal variations resulted in a 41×10^6 m^3 s^{-1} standard deviation. The stream-coordinates estimate of mean absolute transport was found to be about 10% smaller than the corresponding Eulerian mean transport of 146×10^6 m^3 s^{-1} as a result of partially summing the north and south transports within the Mann Eddy, a large semi-permanent anticyclonic eddy normally located just offshore of the NAC. Most transport sections across the NAC in this region include the northward transport of the inshore side of the Mann Eddy because it is difficult to discriminate between the two flows. Historical estimates place the Mann Eddy absolute transport around $50–60 \times 10^6$ m^3 s^{-1}; thus, the transport crossing this transect that can be identified with the NAC is about 90×10^6 m^3 s^{-1}. The barotropic component of the transport (defined as the bottom velocity multiplied by the water depth) is found to contribute at least 30% of the total absolute transport, depending on the choice of baroclinic reference level. Because a time series of transport measurements was made in this study, the accuracy of the mean transport estimate is better than previous estimates, which have all been based on snapshot measurements. From a combination of these measurements with other published measurements, a scheme for the overall circulation and transport in the Newfoundland Basin is suggested.

* Correspondence address: Department of Oceanography, University of Hawaii at Manoa, 1000 Pope Road, MSB 205, Honolulu, HI 96822, USA. Fax: + 1-808-956-9165.

E-mail address: cmeinen@soest.hawaii.edu (C.S. Meinen).

0967-0637/01/$ - see front matter
PII: S0967-0637(00)00103-5

Keywords: North Atlantic Current; Absolute transport; Absolute velocity; Inverted Echo Sounder; IES; Stream Coordinates; Newfoundland Basin

1. Introduction

The Gulf Stream brings warm subtropical waters northward in the North Atlantic. Just west of the Southeast Newfoundland Rise, at about 50°W, it enters a complicated region, where the Gulf Stream transport has been characterized as splitting into three distinct paths (Tomczak and Godfrey, 1994). Some of the flow returns to the west as part of tight recirculation gyres north and south of the Gulf Stream (Hogg, 1992), some travels east–southeast towards the Azores as the Azores Current (Klein and Siedler, 1989), and some of the flow turns northward along the bathymetry to form the North Atlantic Current (NAC) (Mann, 1967; Clarke et al., 1980; Rossby, 1996). There is some controversy regarding how much of the Gulf Stream flow turns to the north and how much of the NAC flow is recirculating in the northern basin independent of the flow of the Gulf Stream (Worthington, 1976; Clarke et al., 1980; Schmitz and McCartney, 1993), which will be discussed in more detail later in the paper. This region is further complicated by the presence of a large (radius ≈ 140 km) anticyclonic Eddy, the "Mann Eddy" (ME), which is nearly always observed just offshore of the NAC near 42°N (Mann, 1967; Clarke et al., 1980; Baranov, 1984; Rossby, 1996). The inshore edge of the ME is often indistinguishable from the northward flowing NAC, and most studies have been unable to separate the two flows (Clarke et al., 1980; Mountain and Shuhy, 1980; Meinen et al., 2000). Finally, inshore of the NAC is the Labrador Current, which flows southward from the Labrador Sea near the shelf break and is thought to partially retroflect somewhere near 41–43°N to travel northward along the inshore edge of the NAC.

Beyond this region, the NAC continues northward through a series of topographically locked meanders (Rossby, 1996) until it reaches about 51°N, where it turns to the east in what Worthington (1976) referred to as the "Northwest corner". Based on hydrographic and drifter studies it appears that all along the northward flowing NAC there is sporadic branching of the NAC with the branches travelling off to the east (Dietrich et al., 1975; Krauss et al., 1987; Klein and Siedler, 1989). At the Mid-Atlantic Ridge (MAR), additional sporadic currents have been observed crossing the Ridge between the main current along the subpolar front and the Azores Current (Dietrich et al., 1975; Krauss et al., 1987; Arhan et al., 1989; Colin de Verdiere et al., 1989).

The importance of the NAC resides in its thermohaline and climatic effects. The NAC transports warm, subtropical waters farther poleward than any other western boundary current, resulting in mild winters for northern Europe (Krauss, 1986; Peixoto and Oort, 1992). In addition to this climatic impact, the NAC also provides the return path for the surface waters that are lost to the deep layer during thermohaline convection in the Labrador, Norwegian, and Greenland Seas (McCartney and Talley, 1984; Tomczak and Godfrey, 1994).

A number of studies have been undertaken in the past to determine the structure and transport of the NAC, but most have been limited to hydrographic sections and the determination of the geostrophic velocity with an assumed level of no motion. The few studies that had absolute velocity measurements demonstrated that assuming a level of no motion, whether at the bottom or at 2000 dbar, resulted in calculated NAC transports that underestimate the true absolute transport by

20–60% (Reiniger and Clarke, 1975; Meinen et al., 2000; Meinen and Watts, 2000). An independently measured absolute velocity reference is thus necessary for the geostrophic method to provide an accurate estimate of the transport. Furthermore, all of these previous studies either have provided only a snapshot of the NAC from a hydrographic section, or have provided an Eulerian time average from moored instruments. While useful, both of these approaches have limitations. Snapshot sections include contamination due to eddies and whatever other short-time-scale processes are present. Eulerian averaging of meandering currents produces a smoothed, broadened, picture of the current (Johns et al., 1995). In order to determine the structure of the NAC, that most accurately represents the snapshot structure independent of other processes, a stream-coordinates approach is adopted.

Several studies have applied stream-coordinates methods to measurements in the Gulf Stream (Halkin and Rossby, 1985; Hall, 1986; Johns et al., 1995; Bower and Hogg, 1996). The details of the stream-coordinates methods used in these studies differ, but the goal is the same: to remove the meandering of the current before applying temporal averaging in an effort to determine a true "snapshot" mean of the current. The study described here will present a stream-coordinates mean of the velocity and temperature structure of the NAC. The estimated transport of the NAC will be based on these velocities and will be compared to historical estimates. The transport will also be put in the context of the overall transport of the entire Newfoundland Basin.

This paper uses data from inverted echo sounders, moored temperature sensors, bottom pressure sensors, and deep current meters deployed across the North Atlantic Current (NAC) near 42.5°N. A "Gravest Empirical Mode" or GEM technique, developed by Meinen and Watts (2000, hereafter MW00), is used to obtain time series of absolute velocity and temperature sections over the period August 1993–February 1995. The experiment was a collaboration between the University of Rhode Island and the Bedford Institute of Oceanography in Halifax, Nova Scotia.

2. Data

Four measurement systems were involved in this study: conductivity-temperature-depth (CTD) profiles, inverted echo sounders that were additionally equipped with bottom pressure sensors, moored temperature sensors, and moored current meters. Fig. 1 shows the locations of the CTDs and the moored instruments. Between July 1993 and July 1995, 191 CTD profiles reaching at least 2000 dbar (1 dbar = 0.1 bar = 10^4 Pa) were obtained; most were full-water-column. Table 1 lists the sources of the CTD data. Six inverted echo sounders with pressure sensors (PIES) were deployed as part of the experiment. Four PIES were recovered with data, although one of the four had a useful travel time record for only the first 3 months. The other three PIES provided full records of acoustic round trip travel time, and all four recorded temperature, and pressure for the full-time period of the experiment, approximately 22 months. Eight tall current meter moorings with up to seven instrumented levels were also deployed; seven moorings with 34 current meters and 37 temperature sensors provided good data over most of the deployment period. Of the seven moorings recovered with good data four had bad speed measurements from the shallowest current meter, so near the core of the NAC the shallowest functional current meters were at a nominal depth of 700 m.

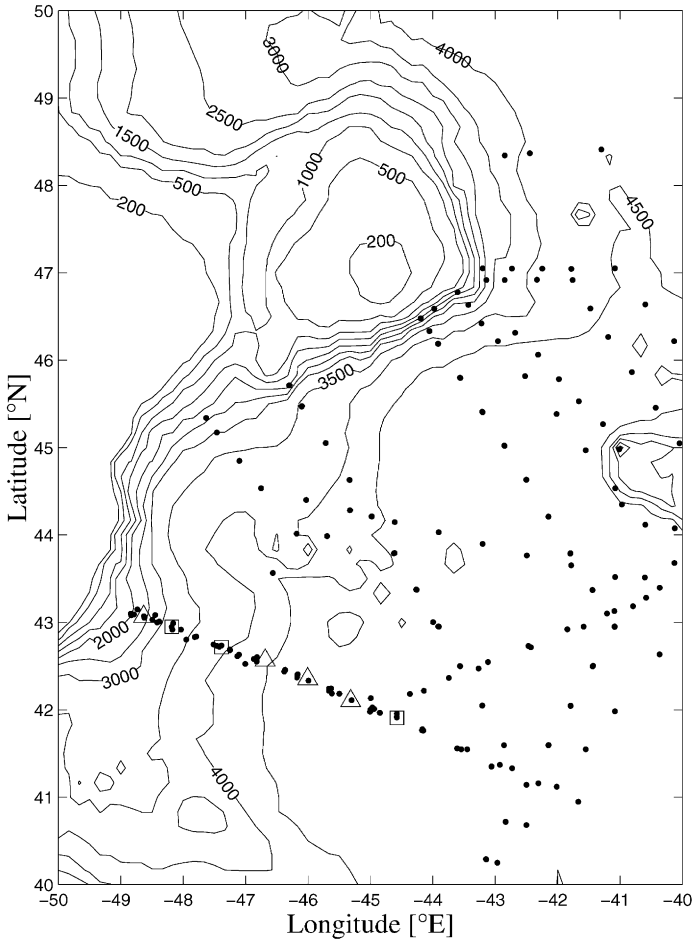

Fig. 1. Locations with moored current meters and temperature sensors (△), and sites with current meters, temperature sensors, and PIES (□). Also plotted are the sites of the 191 full-water-column CTDs used in this study (●).

Table 1
Sources of hydrography used in this study

Source for hydrography	Time of Cruise	No. of casts
German Hydrographic Service	Jul 1993	15
University of Rhode Island	Jul–Aug 1993	31
Bedford Institute of Oceanography	Nov–Dec 1993	49
Bedford Institute of Oceanography	Oct–Nov 1994	50
German Hydrographic Service	Nov 1994	5
Bedford Institute of Oceanography	Apr–May 1995	37
Bedford Institute of Oceanography	Jun–Jul 1993	4

The PIES emits 10 kHz sound pulses and measures the time for these pulses to travel round trip to the sea surface and back. The travel time measurement of the PIES is denoted by τ. All τ time series measured by these instruments were converted into τ time series on a fixed pressure level of 2000 dbar by the methods described in Meinen and Watts (1998). This method takes advantage of empirical linear relationships between τ integrated between the surface and the bottom and τ integrated between the surface and 2000 dbar.

The temperature sensors on each mooring were used to create "pseudo-IES" records following the methods of MW00. Briefly, the procedure uses historical hydrography to determine the dominant temperature profile associated with each particular vertically integrated acoustic travel time, τ, creating a look-up table specific to the region of interest. Reversing the look-up procedure, the several levels of moored temperature measurements at each time step are used to identify a vertical temperature profile, for which the associated τ is the "pseudo-IES" measurement. MW00 presents an intercomparison of "pseudo-IES" estimated τ to PIES measured τ at three sites where current meter moorings were within 1 km of PIES; the RMS difference between the measured and estimated τ values was about 3.5×10^{-3} s. The "pseudo-IES" measurements are used to increase the horizontal resolution between PIES sites and are used interchangeably in all following discussion.

3. Methods

Daily velocity and temperature sections used in this experiment were obtained from the PIESs using the methods described in MW00. A brief review of the method is given here.

3.1. Determining specific volume anomaly and temperature profiles

Because the speed of sound in the ocean is strongly dependent on temperature, the round trip travel time measurement represents a vertical integration of temperature above the PIES:

$$\tau = 2\int_0^p \frac{1}{\rho g c}\,\mathrm{d}p', \tag{1}$$

where ρ, g, c, and p are density, gravity, sound speed, and pressure. MW00 demonstrate a robust empirical relationship between the vertical profile of temperature (or specific volume anomaly) and integrated values of τ. MW00 simulated τ measurements at 2000 dbar via Eq. (1) for 191 CTD casts and then applied smoothing-splines to obtain regular, smooth grids of specific volume anomaly δ (Fig. 2) and temperature T (Fig. 3) as functions of pressure and τ. These fields detail the empirically observed variation of vertical structure, referred to as the "Gravest Empirical Mode" or GEM, as a function of τ. MW00 also demonstrate that the GEM describes more than 95% of the variance of T and δ between 200 and 1500 dbar for this region of the Newfoundland Basin (this depth range was chosen for illustration because it excludes most of the seasonal variability in the near-surface waters and also the greater depths where the real-ocean variability becomes very small). There are similarities between this method and previous attempts to describe the vertical structure of the ocean with analytical flat-bottom modes (Pickart and Watts, 1990), or parallel

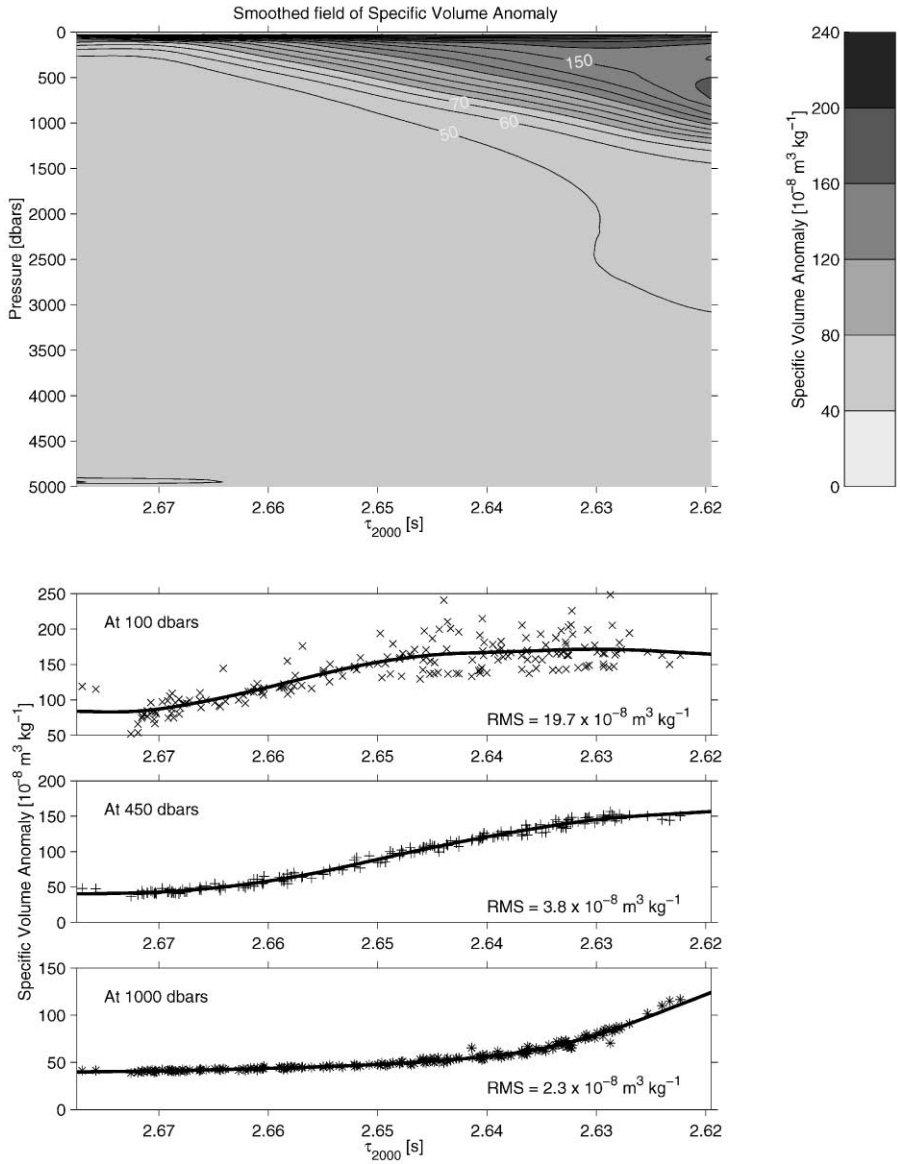

Fig. 2. Smoothed grid of specific volume anomaly as a function of pressure and the simulated round trip acoustic travel time integrated between the surface and 2000 dbar, τ_{2000} (upper panel), developed with data from CTD profiles at locations shown in Fig. 1. Symbols in the lower panels show the CTD calculated specific volume anomaly at several pressure levels as a function of τ_{2000}. Bold lines indicate the specific volume anomaly values from the smoothed field in upper panel. Also noted are the RMS differences at each pressure level. Upper panel modified from Meinen and Watts (2000).

isotherms (He et al., 1998). However, the MW00 method is purely empirical and does not impose any assumptions on the vertical profiles of T or δ.

Larger values of τ represent colder water; thus, the left sides of Figs. 2 and 3 represent waters more often observed on the inshore side of the NAC, with some evidence of the Labrador Current

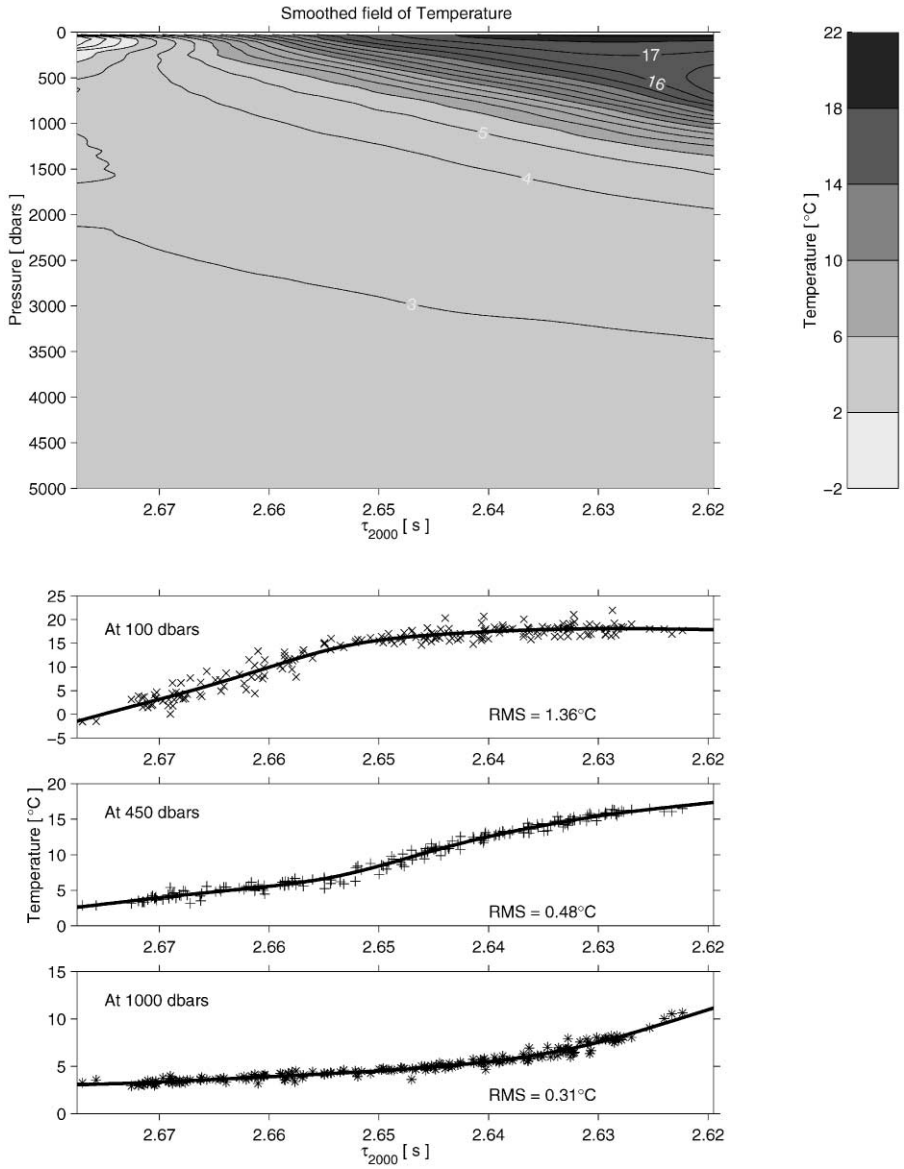

Fig. 3. Smoothed grid of temperature as a function of pressure and the simulated round trip acoustic travel time integrated between the surface and 2000 dbar, τ_{2000} (upper panel), developed with data from CTD profiles at locations shown in Fig. 1. Symbols in the lower panels show the CTD measured temperatures at several pressure levels as a function of τ_{2000}. Bold lines indicate the temperature values from the smoothed field in upper panel. Also noted are the RMS differences at each pressure level. Upper panel modified from Meinen and Watts (2000).

Water with temperatures below 0°C (Fig. 3). The right sides represent the warmer waters usually observed on the offshore side of the NAC. It is important to note that Figs. 2 and 3 represent more than the cross-stream structure of the NAC with τ as the horizontal coordinate; they include all of

the variability from whatever mesoscale eddies and structures were present in the hydrographic measurements. The abscissa represents the entire range of τ that was observed throughout the area of the Newfoundland Basin spanned by the hydrography shown in Fig. 1. Note that there is no spatial connotation to τ; horizontal information is provided only when a pair of PIES provide measurements of τ at specific locations.

To graphically demonstrate how well the GEM structure captures the true ocean variability of T and δ, the lower panels of Figs. 2 and 3 show δ and T versus τ at three pressures (100, 450 and 1000 dbars). The symbols in these panels represent the CTD measured values, and the lines represent the GEM values. The scatter is fairly large at 100 dbars due to seasonal variability, but at 450 and 1000 dbars the scatter about the GEM values is quite small. This confirms that the GEM fields are capturing a majority of the variance at thermocline depths and thus when the GEM fields are combined with PIES measurements it is possible to estimate T and δ with accuracy. As an independent test of the PIES ability to estimate T, MW00 presented a comparison of moored temperature measurements to PIES/GEM estimated temperatures at several sites in the Newfoundland Basin where PIES were within 1 km of current meter moorings. The RMS temperature difference was 0.7°C at thermocline depths and 0.1°C below 1500 m, both small values compared to the true mesoscale ocean variability at those depths (≈ 12 and ≈ 1.5°C, respectively).

3.2. Determining velocities

The look-up relationship $\delta(\tau, p)$ (upper panel, Fig. 2) determines the full-water-column profile of δ from a measurement of τ. Integrating vertically produces a profile of geopotential height anomaly, $\Delta\Phi$. With PIES at two locations, the $\Delta\Phi$ profiles at the two sites can then be differenced horizontally to give a profile of relative velocity, V_{R}, across the span between the two locations via the standard dynamic method. To obtain absolute velocities, an independently measured absolute velocity is needed to provide the reference velocity. For this experiment, the reference velocity was determined by utilizing a leveling procedure that combined bottom pressure measurements from the PIES and velocity measurements from deep current meters (Meinen and Watts, 2000). Maps of absolute bottom pressure along our 1–D section were obtained through optimal interpolation of these two types of measurements (Qian and Watts, 1992; Watts et al., 2001), and reference velocities, V_{btm}, were obtained from the gradients of these bottom pressure maps. Adding these reference velocities to the profiles of V_{R} produces profiles of absolute velocity, V_{absolute}. MW00 present a comparison between directly measured velocities from current meters at several levels to the PIES/GEM derived velocities, which have been absolutely referenced using the deep current meters and bottom pressure sensors as discussed above. The RMS differences between weekly-mean velocities were of 3–5 cm s^{-1}, which is quite good considering the current meters measure point velocities but the PIES-derived velocities represent geostrophic velocities averaged over 50–60 km horizontally.

Using these methods, the combined measurements can be used to obtain complete daily sections of temperature and absolute velocity. These sections were obtained throughout the 19-month period from August 1993–February 1995. Complete details of the technique along with a careful error analysis are found in MW00.

4. Results and discussion

4.1. Sample of daily sections

Fig. 4 shows a selection of the resulting temperature and velocity sections from 6 days during the experiment. The three sections on the left represent days when the NAC appears weak; the three on the right indicate the presence of a strong NAC. A brief description of the velocity structure in each panel follows:

- *November 4, 1993*: On this day, the NAC is centered near 230 km and it appears fairly broad with low-peak velocities of just over 60 cm s^{-1}. There is evidence of a southward flow inshore and below the NAC, but the strongest southward velocities ($|v| > 10$ cm s^{-1}) cover a small portion of the water column. The broadness of the northward flow suggests that the current is crossing the line obliquely (which is confirmed by coincident current meters).
- *February 17, 1994*: The NAC appears narrow enough that the offshore edge of the NAC is contained within the section. There is, once again, moderately strong southward flow inshore of the NAC, and on this day this southward flow appears more barotropic.
- *September 5, 1994*: The core of the NAC is not clearly evident on this day, resulting from the current crossing the section obliquely. There is evidence of the northward flow of the ME on the offshore end of the section.
- *December 29, 1993*: The NAC is located farther offshore on this day than on most days, with a center near 300 km. The peak velocities exceed 100 cm s^{-1}, and the peak bottom velocities exceed 20 cm s^{-1}. Inshore of the NAC there appears to be another northward current, possibly the Slope Water Current (Mann, 1967).
- *June 22, 1994*: The NAC has lower peak velocities here, only 70 cm s^{-1}, and fairly low bottom velocities as well. The ME appears as a distinct northward flow at the offshore edge of the section, one of the few days during the 19-month time series when this distinction is observed. At the inshore edge, the isotherms dome possibly in a cyclonic eddy. This flow reversal might also represent the retroflection of the Labrador Current, although the temperatures do not seem sufficiently low at the inshore edge of the section to justify this hypothesis.
- *February 2, 1995*: On this day, the NAC core is near its strongest, with peak velocities over 160 cm s^{-1}. The inshore edge of the ME completely coalesced with the NAC, and the offshore edge of the ME moved over the outermost moorings with southward velocities greater than 50 cm s^{-1}. There is evidence of a southward, fairly barotropic, flow inshore of the NAC, and over the inshore-most moorings there is the hint of another northward velocity, perhaps the signature of an anticyclonic eddy inshore of the NAC.

Based on these measurements, the NAC evidently meanders and at times crosses the section at oblique angles. Both of these effects cause the Eulerian mean section of a current to appear too broad and reduce the velocities artificially. Both of these problems must be dealt with in order to determine the best "snapshot" mean structure of the NAC.

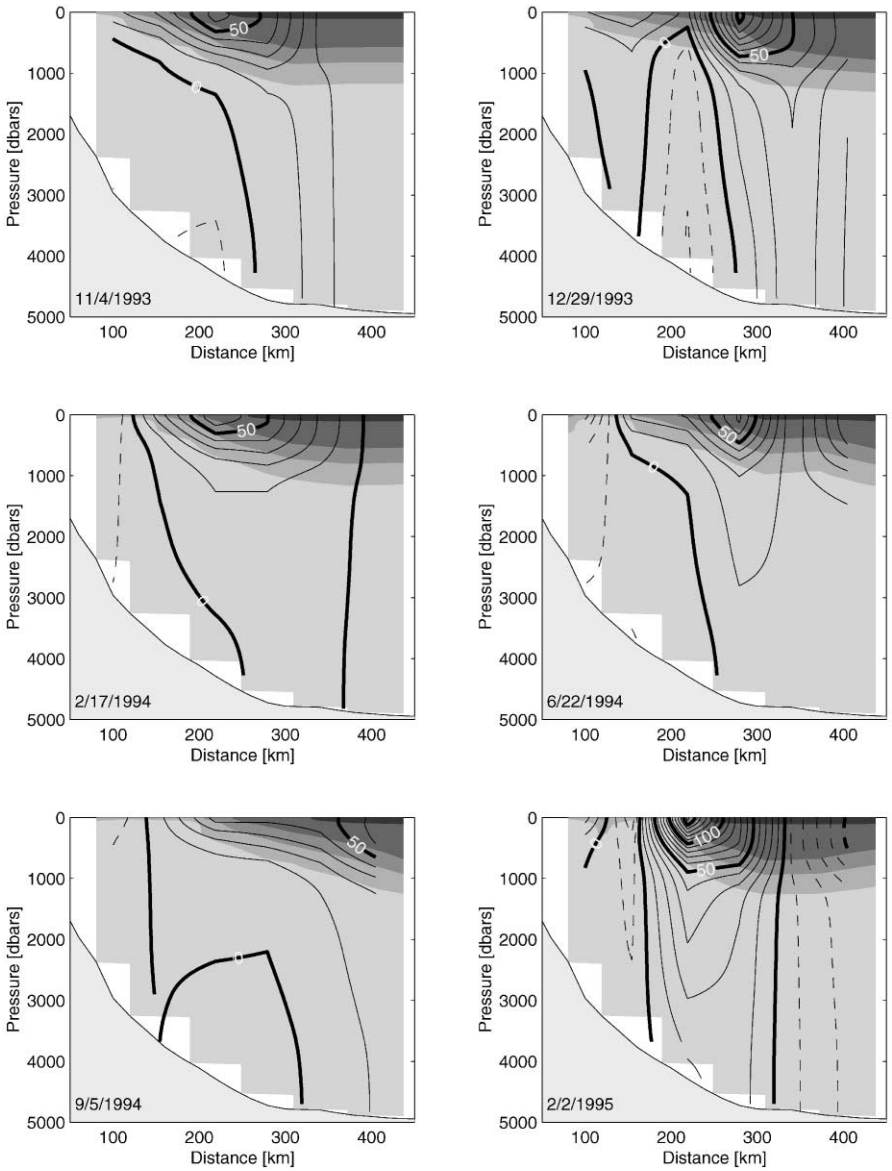

Fig. 4. Six individual temperature and velocity sections at the dates (month/day/year) indicated at lower left of each panel. Gray-scale field denotes temperature at 4°C contour intervals; the deep ocean is between 2 and 6°C. The contour lines are absolute velocity; bold contours are at 50 cm s^{-1} intervals (selected contours labeled in white) and thin contours are at 10 cm s^{-1} intervals. Dashed contours indicate negative (southward) flow.

4.2. Creating stream-coordinates average

The basic idea of the stream-coordinates approach is that a coordinate system is defined wherein the origin is not fixed relative to the local geography, but rather is defined to be fixed to some identifying feature of the center of the current. Different definitions for the center have been used in

the past; the most common choice has been that of a specific isotherm occurring at a specific depth, such as the 12°C isotherm at 400 dbar used by Johns et al. (1995) in the Gulf Stream. For the purposes of this study, the origin was defined as the location where the 10°C isotherm crosses 450 dbar. The final mean stream-coordinate velocity and temperature structures are not particularly sensitive to this choice as long as the isotherm chosen is near the middle of the thermocline and the pressure chosen is near the mid-range of the thermocline excursion across the front.

Based on this definition of the stream-coordinates origin, a time series of the position of the center of the front was generated from the temperature sections calculated with the PIES measurements (Fig. 5, upper panel). The mean position along the line was 252 km from the geographic origin, defined to be where the section crossed the 200 m isobath. The standard

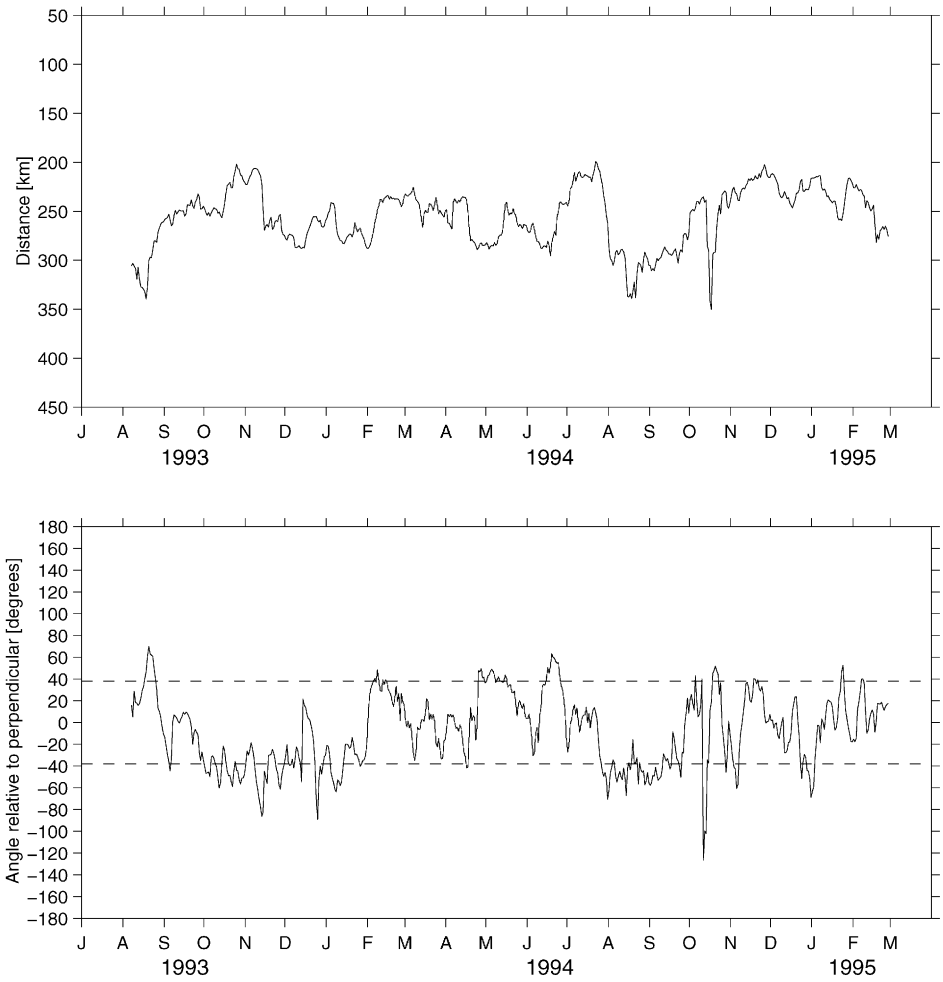

Fig. 5. Top panel: Time series of the position of the center of the current. Current center is defined as the location where the 10°C isotherm crosses 450 dbar. Bottom panel: Time series of the angle with which the current crosses the section, relative to perpendicular, at the center location plotted in top panel. Dashed lines indicate the $\pm 38^{\circ}$ cutoffs where the current was judged to be crossing the section too obliquely to be used in making the stream-coordinates means. Tick marks on lower axis of each panel indicate the beginning of each month.

deviation of the center position was 28 km, and the standard error of the mean was 7 km (the determination of the number of degrees of freedom is discussed in the appendix). Although 28 km is not a large distance compared with the ≈ 150 km width of the NAC, it is large enough that a few significant differences do appear between the stream-coordinates and Eulerian average sections, as will be shown shortly.

This experiment had been designed to cross the NAC at a location where there was minimal meandering and where the NAC was thought to cross the section orthogonally. The small standard deviation of the center of the current indicates at least the former design criterion was correct. Study of the velocity angles measured by the current meters indicates, however, that the current crossed the section occasionally at angles greater than 80°. Fig. 5 (lower panel) shows the time series of the current angle relative to perpendicular, where the current angle was determined for each day by interpolating the velocity angles measured by the top current meters on each of the moorings (nominal depth 400 m) to find the value at the stream-coordinates origin as defined above. Negative angles indicate a crossing angle north of perpendicular; positive angles indicate crossing angles south of perpendicular. The mean angle was $-8°$, or slightly north of perpendicular, so in the mean the current crossed the section nearly orthogonally. The standard deviation of the angle is 33°, however, indicating that significant turning of the current does occur. Recall that the geostrophy-based methods provide only the component of the velocity orthogonal to the section; thus, when the crossing angle is strongly oblique the velocities will be significantly underestimated. To obtain the best possible stream-coordinates structure of the NAC, time periods when the crossing angle was greater than $\pm 38°$, indicating an underestimation of the velocities of greater than 20%, were not used. These cutoffs are denoted by the dashed lines on the lower panel of Fig. 5. About 70% of the time series remained after this subsampling.

4.3. Average stream-coordinates structure

After shifting each daily velocity and temperature section based on the location of the front from Fig. 5, the final step in determining the stream-coordinates mean structure was to average the velocities and temperatures into 20 km bins. Fig. 6 displays the resulting stream-coordinates average structure of the NAC. The top panel displays the average velocity structure, and the bottom panel displays the average temperature structure. The peak velocities in this mean NAC surpass 80 cm s^{-1}; peak bottom velocities exceed 10 cm s^{-1}. The main thermocline, centered near the 10°C isotherm, deepens by about 800 dbar from inshore to offshore over a distance of about 150 km. Fig. 7 shows the Eulerian average structure of the NAC using the same time periods for the averaging. The Eulerian peak velocities only reach 60 cm s^{-1}. The core of the current, defined as velocities greater than 30 cm s^{-1}, increases in width from 150 km for the stream-coordinates average to 170 km for the Eulerian average. The core of bottom velocities greater than 10 cm s^{-1} widens slightly in the stream-coordinates mean. The Eulerian temperature front also appears broader, with less steeply sloped isotherms.

4.4. Temperature and velocity variance

The velocities at 100 and 3000 dbar and the corresponding standard errors of the means are shown in Fig. 8. Only at the core of the current is there a statistically significant velocity difference

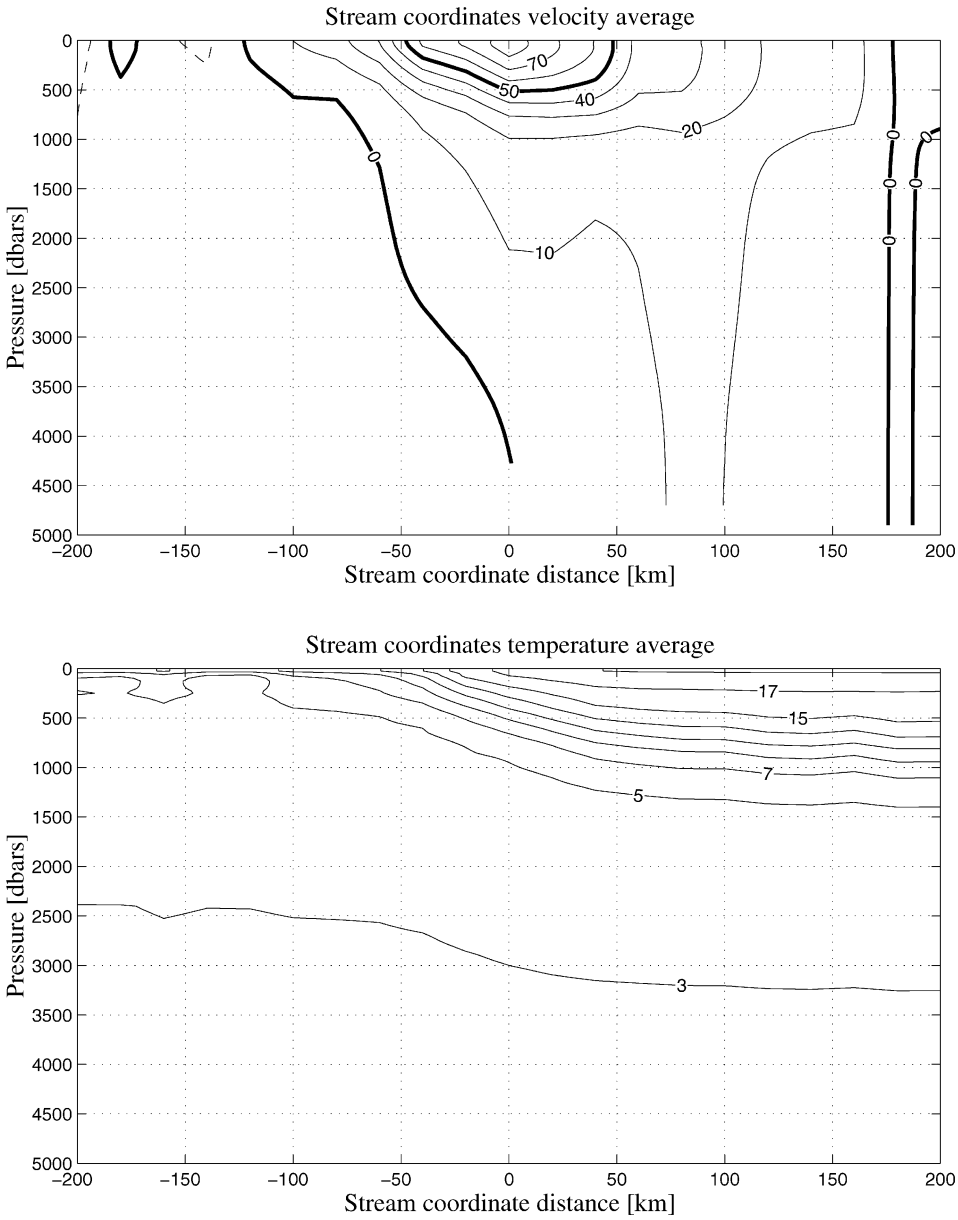

Fig. 6. Stream-coordinates average structure, absolute velocity (top) and temperature (bottom). Velocity contours are as in Fig. 4; temperature contours are at 2°C intervals.

between the two average velocity sections at 100 dbar. At 3000 dbar, there is little difference between the mean velocities. Previous studies have found more obvious differences between stream-coordinates velocity structures and Eulerian velocity structures, probably because they

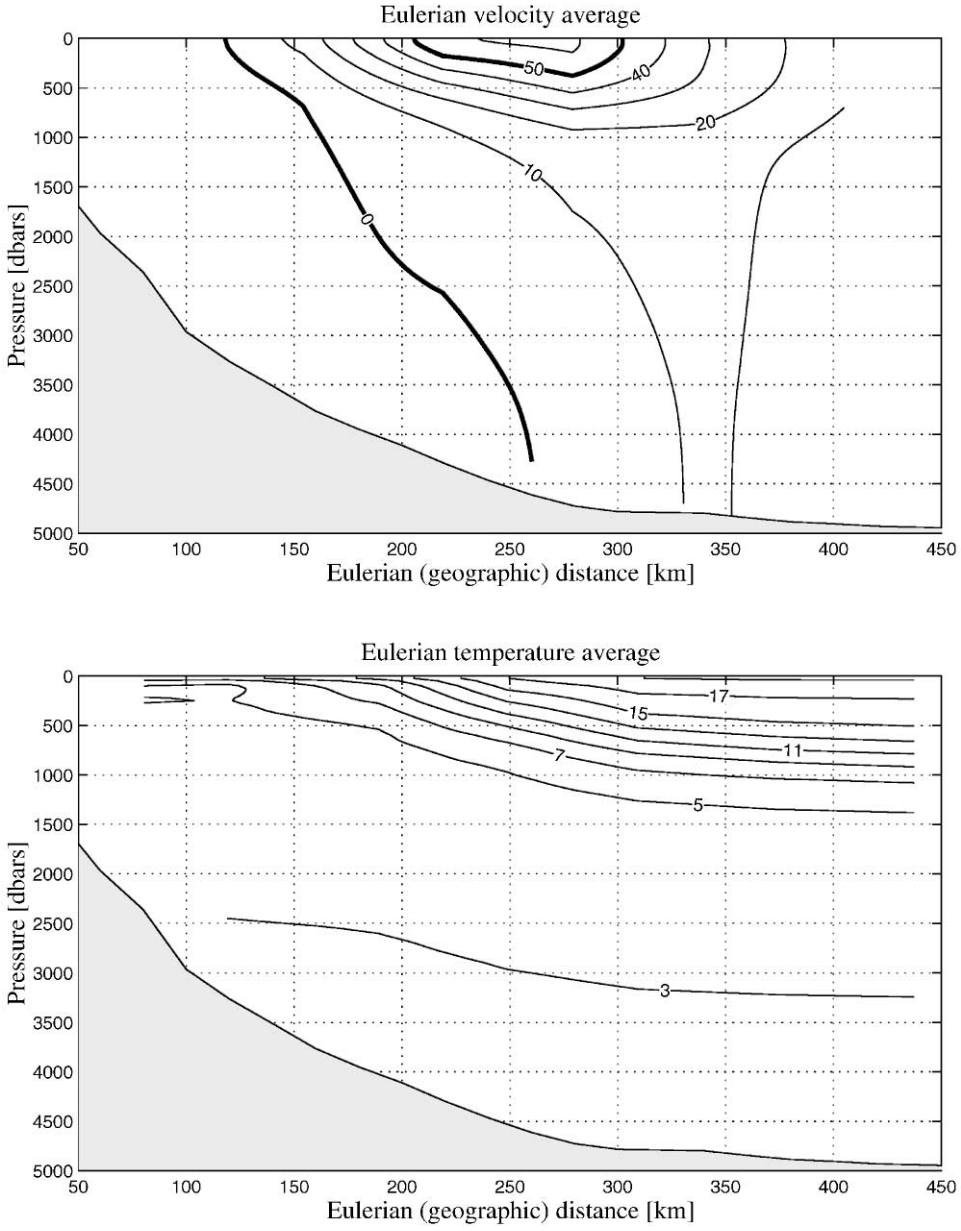

Fig. 7. Same as Fig. 6 except Eulerian averages over same time interval.

were conducted in regions with more vigorous meandering of the current. The study of Johns et al. (1995) found much more significant differences for the Gulf Stream near 68°W; however that study used directly measured velocities from current meters, whereas the present study uses geostrophic velocities, which spatially average between mooring pairs. As such, the latter technique always results in some smoothing of the velocities at the horizontal scale of the mooring pair distance, for

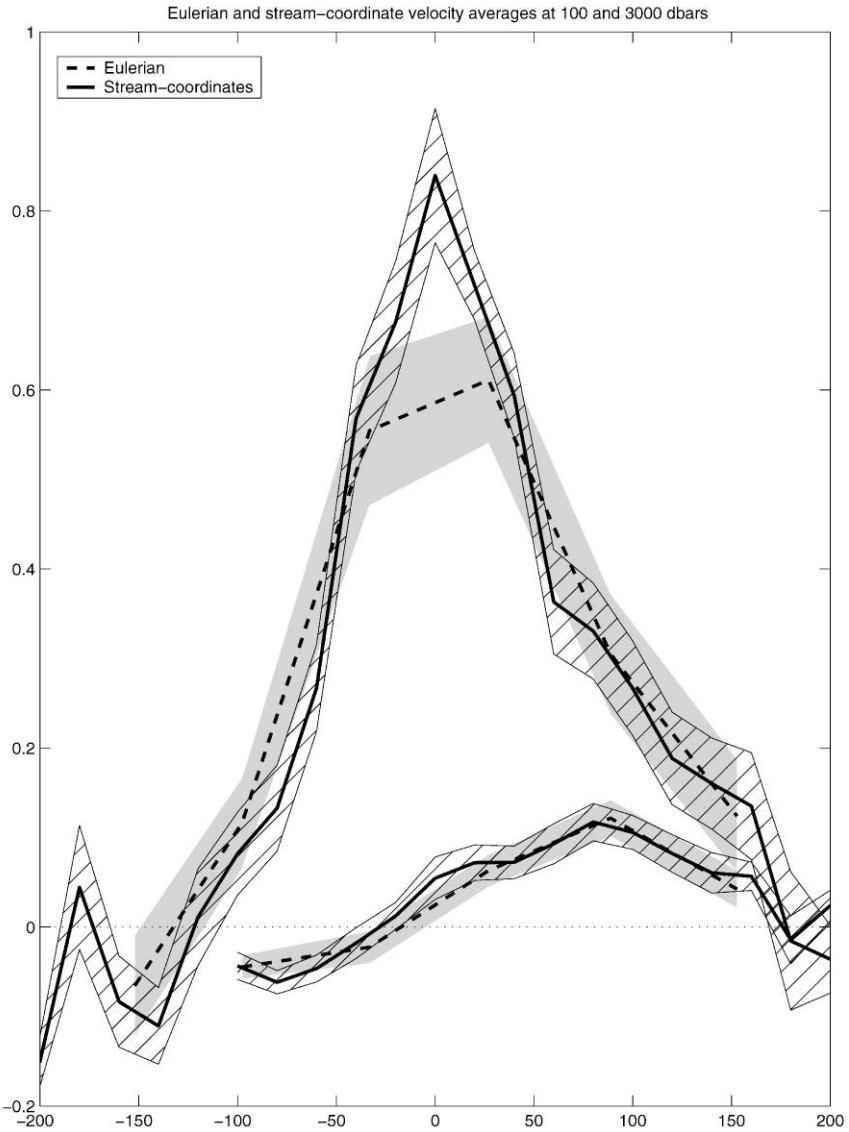

Fig. 8. Stream-coordinates (—) and Eulerian (– – –) velocity cross-sections at 100 and 3000 dbar. One standard error of the mean denoted by cross-hatch for the stream-coordinates velocities and by gray-shading for the Eulerian velocities.

this study 50–60 km. The use of a stream-coordinates mean for these geostrophic velocities, nevertheless, provides a more accurate estimate of the temporal-mean horizontal structure of the NAC than does the Eulerian mean. Based on calculations of variance, it was determined that the meandering of the current accounts for about 35% of the velocity variance at 50 dbar, 18% at 1000 dbar, and 8% at 3000 dbar. The temperature variance shows similar reductions in stream-coordinates.

4.5. Volume transport

The transport of the NAC (including part of the northward ME transport) calculated from the average stream-coordinates velocity section (Fig. 6) is 131 Sv (1 Sv = 10^6 m^3 s^{-1}). The absolute transport can be broken up into two components,

$$\mathrm{Tr_{abs}} = \mathrm{Tr_{bcl}} + \mathrm{Tr_{ref}},$$

where $\mathrm{Tr_{bcl}}$ denotes the baroclinic component relative to a level of no motion and $\mathrm{Tr_{ref}}$ denotes the component due to $V_{\mathrm{ref}} \times H$, where H is the water depth. The baroclinic transport $\mathrm{Tr_{bcl}}$ (relative to a level of no motion at the bottom) is 95 Sv, $\mathrm{Tr_{ref}}$ (using a bottom reference level) is 36 Sv. The standard deviation of $\mathrm{Tr_{abs}}$ is $\varepsilon_{\mathrm{std}} = 41$ Sv, and the statistical standard error of the mean is $\varepsilon_{\mathrm{sem}} = 11$ Sv. Based on the error analysis published in MW00, the measurement error bars for the absolute transports in this method consist of a potential bias $\varepsilon_{\mathrm{bias}}$ of 8.8 Sv and a random scatter error $\varepsilon_{\mathrm{random}}$ of 9.9 Sv for an individual daily section. The bias is not reduced as an error source when a temporal average is taken, but the random scatter is reduced based on the number of degrees of freedom (see the appendix), resulting in an $\varepsilon_{\mathrm{rndavg}}$ of 2.0 Sv for the 19-month average. Because there is no reason to believe that $\varepsilon_{\mathrm{sem}}$, $\varepsilon_{\mathrm{bias}}$, or $\varepsilon_{\mathrm{random}}$ are correlated with one another, the

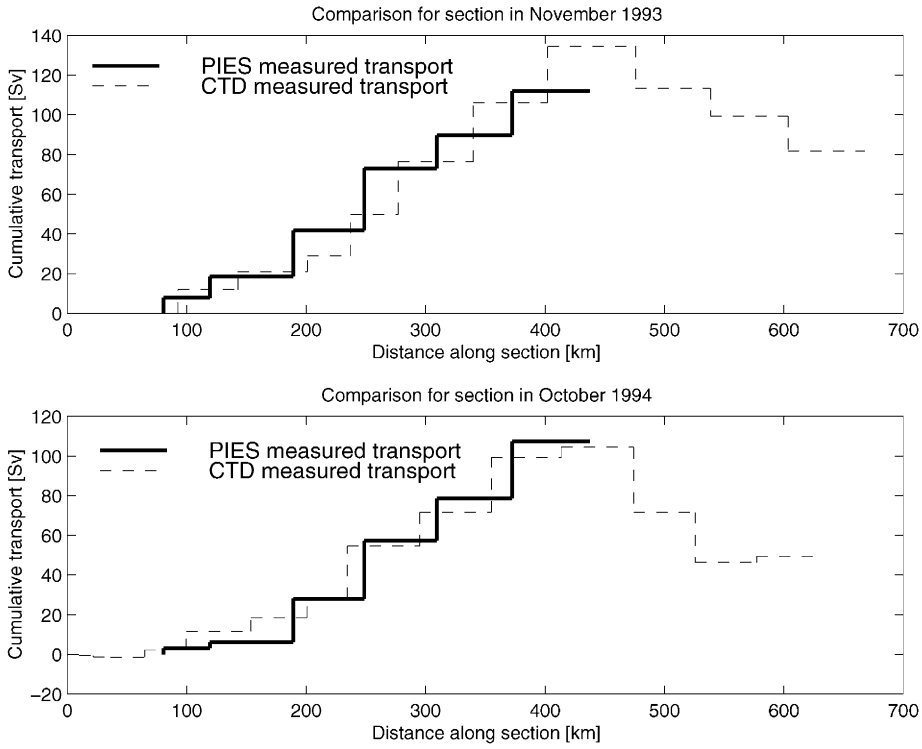

Fig. 9. Cumulative transport relative to a level of no motion at the bottom for a CTD section in November 1993 (top panel) and another CTD section in October 1994 (bottom panel), shown by dashed lines (- - - -). The solid lines (—) indicate the coincident cumulative transport (relative to the bottom) determined by the PIES.

total accuracy of the transport estimates (sometimes called the Mean-Square Error or MSE (Rice 1988; Emery and Thomson, 1997)) is given by the square-root of the sum of the squares of the bias and random error sources. For the time series mean the error is given by $\sqrt{(\varepsilon_{\mathrm{sem}})^2 + (\varepsilon_{\mathrm{bias}})^2 + (\varepsilon_{\mathrm{rndavg}})^2} = \sqrt{11^2 + 8.8^2 + 2.0^2} = 14$ Sv; the measurement accuracy of the daily measurements is given by $\sqrt{(\varepsilon_{\mathrm{bias}})^2 + (\varepsilon_{\mathrm{random}})^2} = \sqrt{8.8^2 + 9.9^2} = 13$ Sv. As a further verification of the accuracy of the transports calculated from this method, two CTD sections, which were obtained along the section while the moored instruments were in place, were used to calculate geostrophic transports relative to a level of no motion at the bottom. Fig. 9 shows the transports calculated on the two cruises and the coincident transports calculated from the PIES. The first cruise was in November 1993 (C.S.S. Hudson cruise number 93039); the NAC $\mathrm{Tr}_{\mathrm{bcl}}$ determined from the CTD section was 135 Sv, and from the moored instruments it was 112 Sv. The second cruise was in October 1994 (C.S.S. Hudson cruise number 94030); the CTD and moored $\mathrm{Tr}_{\mathrm{bcl}}$ estimates were 104 and 107 Sv, respectively. The agreement between the two independent methods is quite good, considering that the locations of the CTD profiles did not exactly correspond to the locations of the PIES and that it took more than two days to occupy all of the CTDs across the current during both of these cruises. Table 2 lists estimates of the transport of the NAC from this and other published historical studies. Transports referenced to levels of no motion at the bottom and at 2000 dbar are also shown in order to compare with other historical estimates. The absolute

Table 2
Estimates of the NAC transport

Source of estimate	Method of calculating transport (Sv)			
	Absolute	Relative to 2000 dbars	Relative to bottom	Barotropic ($V_{\mathrm{btm}} \times H$)
19-*month time series mean transport*				
This study	131 ± 14	57	95	36
MW00	146 ± 14	57	95	51
Instantaneous snapshot estimates				
Meinen et al. (2000)	112 ± 25	59	93	19
Reiniger and Clarke (1975)	123 ± 50	49	—	—
	127 ± 50	50	—	—
	112 ± 50	44	—	—
Clarke et al. (1980)	—	44	78	—
Mann (1967)	—	35[a]	—	—
Worthington (1976)	—	—	74	—
	—	—	97	—

[a]Mann's estimate does not include the transport of the so-called "Mann Eddy" as it was distinguishable from the NAC during his study.

MW00 reported the Eulerian mean from this experiment. Meinen et al. (2000) used POGO and ADCP measurements to reference a geostrophic shear section from CTD measurements. Reiniger and Clarke (1975) used 24 h averages from moored current meters to reference three separate geostrophic shear sections from CTD sections. Clarke et al. (1980), Mann (1967), and Worthington (1976) worked solely with unreferenced geostrophic shear sections based on CTD measurements.

transport estimate is within $\pm$ 25 Sv of the other absolute transport estimates that have been made at this location. The baroclinic transports calculated relative to levels of no motion at the bottom and 2000 dbar also compare favorably with the historical estimates made by Worthington and others.

4.6. Barotropic–Baroclinic transport breakdown

As mentioned previously, most historical measurements of ocean current transports have been based on the assumption of a level of no motion, a well-known problem. The measurements made in this experiment provided an opportunity to study the relationship between the Tr_{bcl} and Tr_{ref} components (the latter here defined as $V_{btm} \times H$) of the NAC (Fig. 10). This comparison was made for the net transport across the section, which includes the NAC, ME, and DWBC transports, as well as for the northward component only, which includes the NAC and ME.

The comparison for the net transport across the section (Fig. 10, upper panel) shows that Tr_{bcl} varies only a small amount, although the peak-to-peak variations are statistically significant based on the estimated errors, with a mean of 95 Sv and a standard deviation of 15 Sv. This is consistent with the experimental design, which placed the mooring line at this location because hydrography-based baroclinic transport snapshots had suggested that a short line of moorings could consistently capture the transport of the NAC at this location. Tr_{ref}, which was transparent to the historical hydrographic studies, varies much more than Tr_{bcl}: the mean Tr_{ref} was 17 Sv and the standard deviation was 39 Sv. The variability of Tr_{ref} dominates the variability of Tr_{abs}, as can be shown by calculating the sample correlation coefficients, r, between each of the components and Tr_{abs} (Bendat and Piersol, 1986). There is a significant correlation between Tr_{ref} and Tr_{abs}, $r = 0.95$, but the correlation between Tr_{bcl} and Tr_{abs} is much lower, $r = 0.57$. Tr_{ref} and Tr_{bcl} are only weakly correlated with one another, with an r value of only 0.29. Neither of the latter two correlations are significantly different from zero at two standard deviations. This indicates that, at least for this region, no consistent relationship exists between the Tr_{ref} and Tr_{bcl}.

One might hope that while there was no relationship between Tr_{bcl} and Tr_{ref} components of the net transport across the section, there might be a relationship in the NAC, which is a single dynamical feature. The integration over the northward components only (Fig. 10, lower panel) is strongly dominated by the NAC and the inshore edge of the ME, although other circulations such as the aforementioned Slope Water Current or cyclonic eddies inshore of the NAC could have some influence on the integral. The integration demonstrates that the northward component of Tr_{bcl} remains fairly constant throughout the experiment, with a mean value of 100 Sv and a standard deviation of 14 Sv. The variability of the northward Tr_{ref}, with a 34 Sv standard deviation, again overwhelms the variability of Tr_{bcl}. The correlations for these northward transports are virtually the same as for the net transport measurements: strong correlation between the Tr_{ref} and Tr_{abs} but no significant correlation between either the Tr_{ref} component or Tr_{abs} and the Tr_{bcl}.

4.7. Transport variability

There are some surprising transports measured during the time series. For periods of about a week in November 1994 and January–February 1995 the net transport across the section is southward, which serves to highlight the variability and complicated nature of this region. Fig. 10

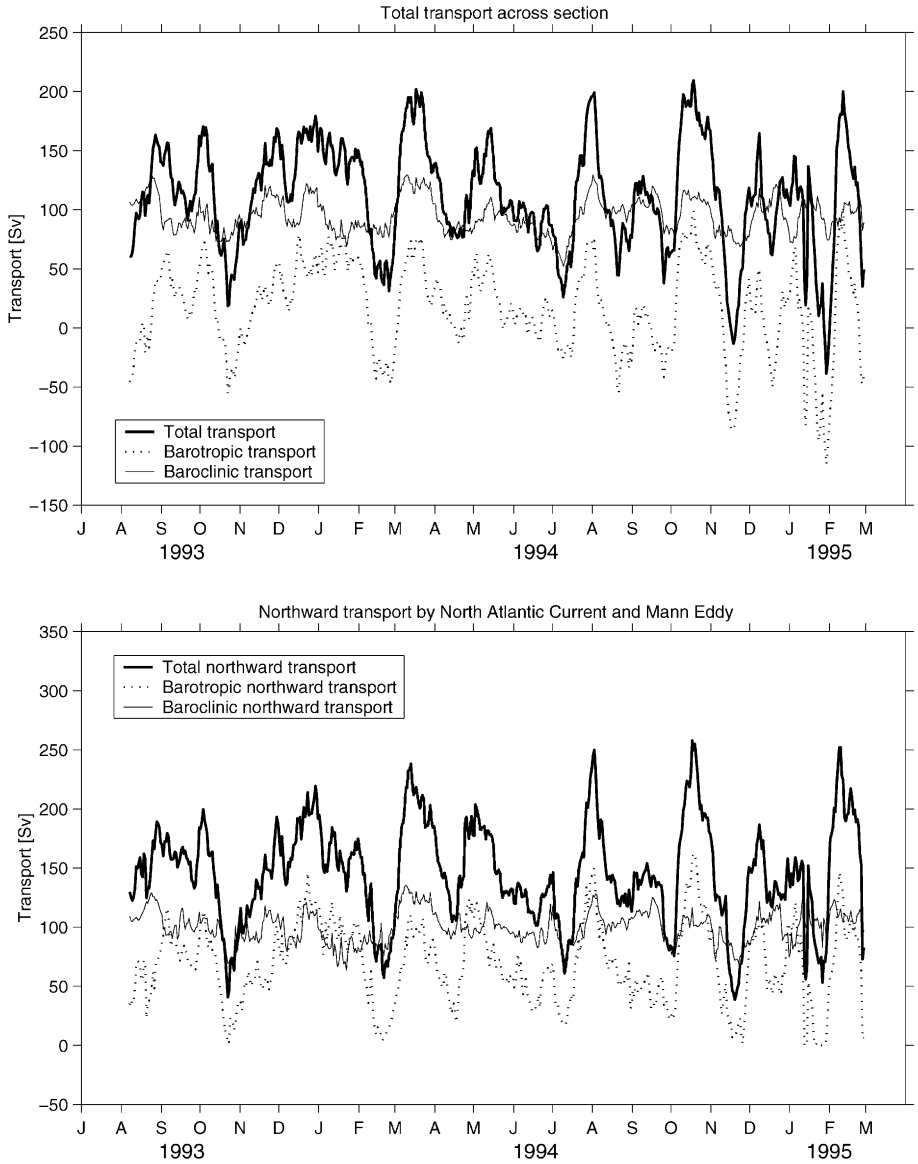

Fig. 10. Variation in the transport across the section over the 19-month time series. Top panel shows the net transport across the complete section broken into baroclinic (relative to a level of no motion at the bottom) and barotropic (bottom velocity multiplied by depth) components as well as the total transport. Bottom panel shows only the northward component of the transport offshore of 125 km. Tick marks on lower axis indicate the beginning of each month.

seems to indicate a large amount of variability in the transport entering the Newfoundland Basin via the NAC. A simple "back of the envelope" calculation indicates that the net inflow from the south into the Newfoundland Basin cannot indeed be varying quite so widely. Assuming an approximately 2000 km × 2000 km area for the North Atlantic Ocean north of 40°N, and

assuming an increase in transport of 40 Sv for a week, the resulting sea-level change would be about 6 m. Even a small fraction of this change would be easily observed by tidal stations. Thus, the vast majority of the transport variability observed along our section, with a standard deviation of about 40 Sv, must be compensated by flows inshore and offshore of our section.

The high-frequency transport variability is reduced with 3-month temporal averaging, as illustrated in Fig. 11. Each different symbol represents a 3-month period (circles represent

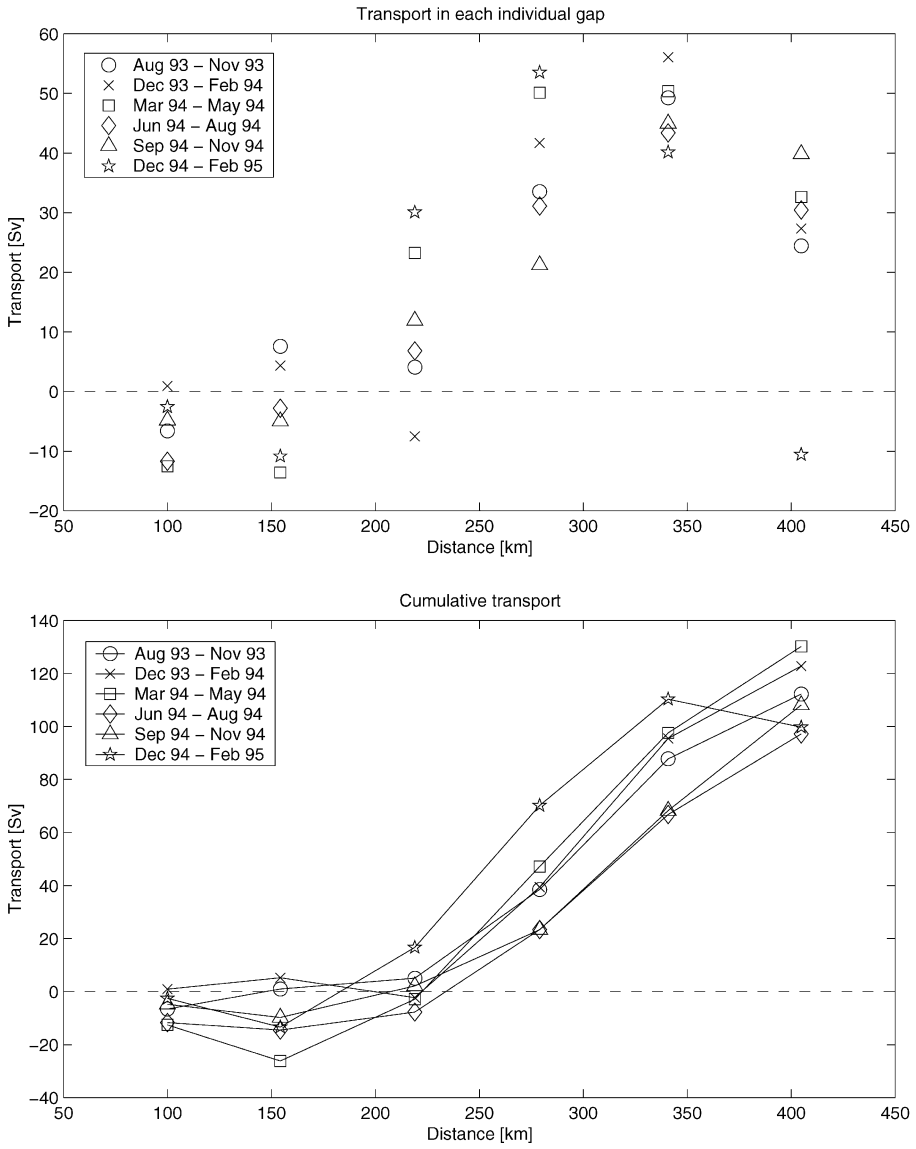

Fig. 11. Three-month-average transports calculated both independently in each gap between moorings (top panel) and as a cumulative integral from the western end of the section (bottom panel). Time periods associated with each symbol noted in legend. Distance measured from 200 m isobath.

a 4-month period) roughly corresponding to seasonal intervals. In the top panel, the transport calculated independently in each gap is denoted; the lower panel shows the cumulative transport integrated from the west end of the section. The meandering of the NAC results in widely scattered measured transports at the gaps centered near 220 and 280 km, where the transport varies by 25–40 Sv. The meandering also causes the shifting of the peak in the cumulative transport between 340 and 410 km. Essentially, however, the structure of these transports is fairly consistent from season to season without any apparent seasonal trend. The total cumulative transport varies by about 30 Sv between various seasons.

At the gap centered near 410 km the scatter is quite large, primarily due to the winter 1994–1995 season, when the transport becomes negative. Recall from Fig. 4 that during February 1995 the inshore edge of the ME had completely coalesced with the NAC and the southward flowing offshore edge of the eddy was observed at the outer edge of the section. This southward flow results in the negative transport noted for the winter months. The cumulative transport for that winter shows a decrease in total transport at the end of the section, but the peak northward transport falls near the middle of the peak transports from the other time periods. The opposite extent of the MEs motion occurs during the summer 1994 season. Fig. 4 showed that during late June 1994 the ME had moved offshore and the northward peak of the ME velocity was distinguishable from the northward flow of the NAC. The cumulative transport across the section during the summer 1994 season is the lowest of the entire time series, indicating that less of the ME transport crossed the section.

Inshore of the NAC there is a consistent southward flow in the mixed-water regime ranging in size between 8 Sv (fall 1994) and 27 Sv (spring 94). In winter 1993–1994, however, the flow in the two inshore-most gaps reverses sign and becomes northward. Fig. 4 showed this northward flow on December 29, 1993. It is impossible to assess definitively the exact cause for this northward flow, but a plausible explanation would be that it results from the Slope Water Current. Mann (1967) and Clarke et al. (1980) have shown evidence for an additional current flowing eastward north of the Gulf Stream at about 50°W. This current, commonly referred to as the Slope Water Current, is believed to combine with the Gulf Stream prior to the Gulf Stream splitting at the Southeast Newfoundland Ridge and forming the NAC. A possible explanation for the northward flowing water observed during the winter of 1993–1994 by our section is that during this period the Slope Water Current maintained a unique identity and rounded the ridge, not coalescing with the NAC until after it passed our section. The 5–9°C temperatures observed by the PIESs at 200 dbar are consistent with the temperatures observed in the Slope Water Current by Clarke et al. (1980), which lends confidence to this interpretation. During the same period, an anomalous strong southward transport was observed centered near 220 km; based on this and the velocity sections from this time period (Fig. 4) it appears that the southward flow of the Deep Western Boundary Current (DWBC) had moved farther offshore than was observed during the rest of the experiment.

4.8. *Stream coordinates*: *effects of the Mann Eddy*

One surprising result of this experiment was that the transport of the NAC calculated in stream-coordinates, 131 Sv, was *smaller* than the 146 Sv calculated in Eulerian coordinates by MW00. The Gulf Stream study of Johns et al. (1995) found a 30% increase in transport when calculated in stream-coordinates, attributed to the presence of recirculation gyres on both sides of

the current; meandering of the current and these associated recirculations reduced the transport when it was calculated in Eulerian coordinates. Although the 10% decrease observed for the NAC when calculated in stream-coordinates is small, it is slightly larger than the estimated error bar for the Eulerian mean section and as such requires some explanation. (Keep in mind that because the same measurements were used in developing the two mean velocity sections, the difference between the sections need only be larger than the 14 Sv error bar of one of the sections to be significant, not larger than $\sqrt{14^2 + 14^2} = 20$ Sv.)

The Mann Eddy is the key to the different result in our study. As mentioned previously, the inshore edge of the ME contributes a significant portion of the measured transport attributed to the NAC. The ME is normally directly adjacent to the NAC, but at times it moves 50 km or more away from the NAC. Because the stream-coordinates origin is defined as the center of the NAC, the shifting of the coordinates system in a manner not tightly correlated to the location of the ME results in a smearing of the isotherms and isotachs associated with the ME. In particular, because the offshore portion of the ME, flowing southward, gets averaged into the whole, the result is a reduction of the transport of the ME, and thus the NAC. Tests using a simple kinematic model with a sinusoidal velocity structure that decays exponentially with depth confirms this hypothesis, yielding a decrease in transport of more than 10% for reasonable combinations of parameters. Because we cannot quantify precisely how much this process reduces the transport for the real ME, we will proceed by using the Eulerian transport for the NAC + ME in the following discussion of the overall circulation of the Newfoundland Basin.

5. Circulation of the Newfoundland Basin

Reiniger and Clarke (1975) obtained estimates of 12, 55, and 61 Sv for the absolute transport of the ME using three separate CTD-derived geostrophic relative velocity profiles referenced with current meters. These are the only estimates of the absolute transport of the Mann Eddy, and from the magnitude of the baroclinic signal I suspect the estimate of 12 Sv was missing a significant portion of the total transport. A preliminary study of hydrography gathered in the Newfoundland Basin during 1972 and also during 1993–1995 indicates that the baroclinic transport, relative to a deep level of no motion, may have strengthened since the 1972 measurements of Reiniger and Clarke (1975) (R. Allyn Clarke, pers. comm., 1998). No quantitative information, however, is available on the magnitude of this change, and no data are available on changes in the deep velocity and the associated component of the transport. For the purposes of this paper, therefore, it shall be assumed that the ME carries about 50–60 Sv; thus the throughput transport of the NAC is about 90 Sv at 42.5°N. In order to get a more accurate estimate of the NAC throughput it would be necessary to measure the absolute current structure along a line that extended across the entire ME and any other recirculation that may exist in the Newfoundland Basin.

Consider the northwest North Atlantic, north of 40°N and west of the Mid-Atlantic Ridge (MAR), as a box within which volume is conserved. Our study indicates about 90 Sv enters the basin from the southwest corner in the NAC, and the work of Schmitz and McCartney (1993) indicates that about 10 Sv enter in the Deep Northern Boundary Current (DNBC) from the north and as Antarctic Bottom Water from the south. Our study shows about 30 Sv exits the basin, to the south, inshore of the NAC. On the east side of the basin, we have a fairly robust estimate of

$\approx$ 30 Sv transport crossing the MAR relative to a level of no motion at the bottom; this transport may be carried in multiple current branches (Krauss, 1986; Krauss et al., 1987). Current meter studies (Arhan et al., 1989; Colin de Verdiere et al., 1989) and inverse analysis studies (Sy, 1988; Sy et al., 1992) indicate that the barotropic component of the NAC as it crosses the MAR is negligible. Thus, for simple mass-balance reasons the $\approx$ 40 Sv excess input via the NAC compared to what exits over the MAR and inshore of the NAC must somehow be leaving the basin. Here are a number of possible pathways:

Ekman transport: Based on the wind fields published by Hellerman and Rosenstein (1983), the annual mean wind stress across the basin is eastward with a magnitude of about 0.15 N m^{-2}. The corresponding southward Ekman transport at 42.5°N due to this wind stress is about 2 Sv, which is too small to be a significant contributor to balancing the mass flow.

Entrainment into the DWBC: Schmitz and McCartney (1993) described the circulation in the North Atlantic using historical hydrographic data and other direct measurements. Based on their analysis, a net transport of about 7 Sv overflows the Iceland–Shetland and Denmark Strait sills (the former waters crossing the MAR through the Charlie Gibbs Fracture Zone) into the northern part of the western North Atlantic basin. These waters form the beginning of the DNBC. An additional 3 Sv of Antarctic Bottom Water enters the Newfoundland basin from the south. Schmitz and McCartney (1993) report further that at the Southeast Newfoundland Rise about 16 Sv leaves the Newfoundland Basin in the DWBC. This indicates that about 6 Sv of the water brought into the basin by the NAC is transformed within the basin, eventually departing through the DWBC. This transformation of 6 Sv is fairly small compared to the 40 Sv difference we are considering.

Recirculation inshore of the NAC: The mean observed southward transport inshore of the NAC was 28 Sv, somewhat larger than the value quoted by Schmitz and McCartney (1993) for the DWBC. It cannot be assessed with this data set whether these measurements indicate that in addition to the DWBC there is recirculation west of the NAC, or that the DWBC transport at this location has been underestimated. The velocities observed inshore of the NAC are fairly barotropic, and therefore would not have been observed by historical hydrographic studies in this region. The larger southward transports are consistent, however, with the $\approx$ 40 Sv estimates of the transport of the subpolar gyre's western boundary current made in the Labrador Sea (Clarke, 1984; Lazier and Wright, 1993). Even if $\approx$ 20 Sv of the southward flow observed inshore of the NAC is recirculating northward on the inshore edge of the NAC, there is still a significant imbalance in the transport entering and leaving the basin.

Recirculation east of the NAC: Lozier et al. (1995) present evidence that there is deep recirculation from the NAC which travels southward all the way around the Sargasso Sea as a large recirculation gyre for the Gulf Stream–NAC system. The southward velocities required to close the transport are quite small: throughout the Newfoundland basin east of the moorings of this study it would require a net southward barotropic (vertically averaged) recirculation of between 0.2 and 0.6 cm s^{-1}. Krauss (1986) did not show any significant southward trend in the velocities measured by his surface drifters in this region, but such small southward velocities would be difficult to resolve with drifters in a region with such high eddy variability (Schmitz, 1981; Richardson, 1983; Baranov, 1984).

At the point where the NAC has reached the Northwest corner near 51°N, the transport has dropped to 50–60 Sv (Lazier, 1994). When the NAC reaches the MAR the transport has dropped to 30 Sv (based on the assumption of an insignificant barotropic component) (Krauss, 1986). This

suggests that a slow loss of water to recirculation southeast of the NAC throughout the path from 42.5°N to the MAR is a plausible explanation for the drop in transport.

5.1. Origin of the NAC waters

Worthington (1976) presented the controversial idea that the NAC represented the western boundary current for a gyre completely independent from the subtropical Gulf Stream gyre. Worthington's hypothesis was that all of the Gulf Stream waters either recirculated directly to the south or crossed the Atlantic basin in the Azores Current. The motivation for this scheme was that the oxygen signal in the deep NAC was significantly different from that of the deep Gulf Stream. Clarke et al. (1980) argued that mixing with the surrounding waters could explain the oxygen difference and that the Gulf Stream was the source for the NAC. Recently, Schmitz and McCartney (1993) have presented a hybrid scheme in which 12 Sv of the Gulf Stream waters turn north to feed the NAC while the rest of the NAC flow is maintained by a recirculation gyre in the Newfoundland Basin. All these competing schemes have been primarily based on the baroclinic transport estimates because of the lack of absolute transport measurements. The absolute transport estimates obtained in this study provide motivation for revisiting this topic.

If the 50–60 Sv estimate of the Mann Eddy absolute transport from Reiniger and Clarke (1975) is representative of the true mean transport of the eddy, then on average the NAC is carrying about

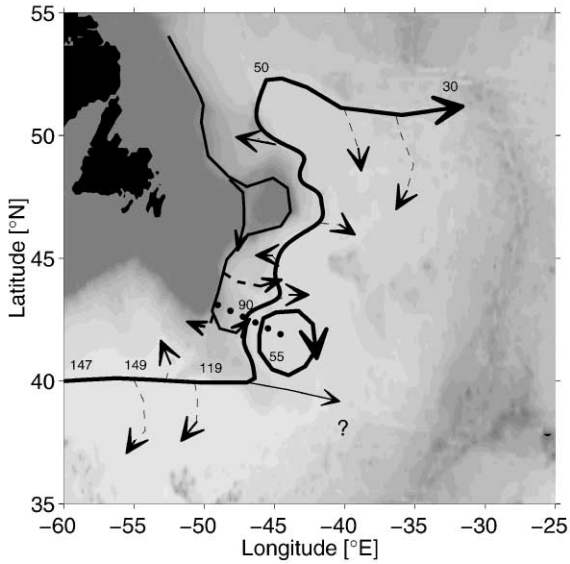

Fig. 12. Cartoon showing the circulation and absolute transport in the Newfoundland Basin. Numbers denote the transport of the Gulf Stream/North Atlantic Current at those locations (in Sv); an estimate of the Mann Eddy absolute transport is also shown. See text for sources of measurements. Bulleted line (●●●●) near 42°N, 46°W denotes mooring line from this experiment. Bold (—), medium (—), and thin (—) lines denote the Gulf Stream/North Atlantic Current, the Labrador Current, and the Azores Current, respectively. Thin dashed (- - - -) and dotted lines denote recirculations or other fluid losses from the Gulf Stream/North Atlantic Current and Labrador Current, respectively. Question mark indicates the Azores Current transport is poorly known in the western basin. Gray-shading indicates ETOPO5 bathymetry, with black shading indicating land.

90 Sv northward at 42.5°N. This water must originate somewhere; it is difficult to imagine that anything approaching 90 Sv could be flowing westward south of the ME in order to supply the NAC as would be required by Worthington's (1976) scheme. Indeed, this flow would be counter to the Azores Current, which flows eastward at that latitude (Klein and Siedler, 1989). The only other reasonable source for most of this volume of water is the Gulf Stream. Measurements of the Gulf Stream absolute transport at 60°W and 55°W appear fairly constant at 147–149 Sv (Hogg, 1992). Reiniger and Clarke (1975) obtained a snapshot estimate of 119 Sv for the Gulf Stream absolute transport at 50°W using hydrography referenced by current meters. While there appear to be significant losses in transport between 55°W and 50°W due to the recirculation gyres north and south of the current, the remaining 119 Sv could provide the majority of the 90 Sv NAC while still providing the transport of the Azores Current and possibly a small amount of remaining recirculation between 50°W and the Southeast Newfoundland Rise. Fig. 12 presents a new circulation scheme for the Newfoundland Basin based on these absolute transport measurements. I hope that, by the postulation of this scheme, gaps in our knowledge will be evident, that further useful locations for measuring the absolute transport will be identified, and that the scheme will be improved and constrained with future measurements.

Acknowledgements

The author completed this work as part of his Ph.D. dissertation at the University of Rhode Island while studying with Dr. Randy Watts. Dr. Watts provided many helpful comments and suggestions for this paper and his help is greatly appreciated. The author would also like to thank Karen Tracey and Mike Mulroney, who helped with the collection and initial processing of the CTD, current meter, and PIES data. Ms. Tracey also provided a number of helpful comments on an early version of the article. Thanks also to the officers and crews of the R. V. *Oceanus* and the C. S. S. Hudson for their work during the deployment and recovery cruises. Dr. Tom Rossby at the University of Rhode Island provided some of the CTD measurements used in this experiment. Dr. Peter Koltermann of the German Hydrographic Survey also provided a number of CTD measurements. Dr. R. Allyn Clarke of the Bedford Institute of Oceanography, Halifax, Canada, provided the current meter records and some of the CTDs used herein. The anonymous reviewers made several helpful suggestions for improving this article. Funding for the Oceanus time, additional current meters and the deployment of the PIES was provided by the Office of Naval Research Contract no. N0001492J4013. Grant number NA56GP0134 from the National Oceanic and Atmospheric Administration provided funds for analysis of the data. The author was funded during the early part of the experiment on an Office of Naval Research (Secretary of the Navy) graduate fellowship and completed his Ph.D. degree under funding from the National Oceanic and Atmospheric Administration. The article was completed while the author was at the University of Hawaii at Manoa.

Appendix. Number of degrees of freedom

The velocity and temperature measurements from day to day are not independent, since the time scales of the major processes in this region are much longer than 1 day. The first step to find the

number of degrees of freedom is to integrate the autocovariance of the record as a function of time lag to find the true variance of the mean (Bendat and Piersol, 1986).

$$\mathrm{Var}(\hat{\mu}_x) = \frac{1}{T^2}\int_{-T}^{T}(T - |\gamma|)C_{xx}(\gamma)\,\mathrm{d}\gamma,$$

where $\hat{\mu}_x$ is the sample mean, T is half the length of the time series, γ is the time lag, and C_{xx} denotes the autocovariance function. The resulting variance of the mean is divided by the variance of the time series determined assuming that each of the individual measurements are independent, resulting in the true number of degrees of freedom in the time series

$$\text{Degrees of freedom} = \frac{\mathrm{Var}(\hat{\mu}_x)}{\mathrm{Var}(x)}.$$

Following this method, the number of degrees of freedom was determined for each of the PIES and pseudo-IES records. With the exception of the inshore-most mooring, this method indicated about 22 degrees of freedom were obtained in the time series. Thus, for our 19 month time series we observe that the water motions have a 13 day integral time scale.

$$\text{Integral time scale} = \frac{1}{2}\left(\frac{\text{Length of record}}{\text{Degrees of freedom}}\right).$$

This is comparable to the 10 day integral time scale found by Johns et al. (1995) for the Gulf Stream using current meters moored at about 400 dbars. Johns also found that the correlation scales for the stream-coordinates system were similar to those for the Eulerian system. This result was assumed to be true for the NAC also, and the same number of degrees of freedom were used for both Eulerian and stream-coordinates quantities. Because about 30% of the time series is excluded in determining the averages (due to the current crossing the line obliquely), the actual number of degrees of freedom used to estimate uncertainties is $0.7 \times 22 = 15$.

References

Arhan, M., Colin de Verdiere, A., Mercier, H., 1989. Direct observations of the mean circulation at 48°N in the Atlantic Ocean. Journal of Physical Oceanography 19, 161–181.

Baranov, E.I., 1984. A quasi-stationary anticyclone eddy and its role in the formation of the Newfoundland Energy-Active Zone. Meteorologiya i Gidrologiya 10, 87–93.

Bendat, J.S., Piersol, A.G., 1986. Random Data. Wiley, New York.

Bower, A.S., Hogg, N.G., 1996. Structure of the Gulf Stream and its recirculations at 55°W. Journal of Physical Oceanography 26, 1002–1022.

Clarke, R.A., 1984. Transport through the Cape Farewell — Flemish Cap section. Rapports et Proces-Vertaux des Reunions, Conseil International pour l'Exploration de la Mer 185, 120–130.

Clarke, R.A., Hill, H.W., Reiniger, R.F., Warren, B.A., 1980. Current system south and east of the Grand Banks of Newfoundland. Journal of Physical Oceanography 10, 25–65.

Colin de Verdiere, A., Mercier, H., Arhan, M., 1989. Mesoscale variability from the western to eastern Atlantic along 48°N. Journal of Physical Oceanography 19, 1149–1170.

Dietrich, G., Kalle, K., Krauss, W., Siedler, G., 1975. General Oceanography. Wiley, New York.

Emery, W.J., Thomson, R.E., 1997. Data Analysis Methods in Physical Oceanography. Pergamon Press, Oxford.

Halkin, D., Rossby, H.T., 1985. The structure and transport of the Gulf Stream at 73°W. Journal of Physical Oceanography 15, 1439–1452.

Hall, M.M., 1986. Horizontal and vertical structure of the Gulf Stream velocity field at 68°W. Journal of Physical Oceanography 16, 1814–1828.

He, Y., Watts, D.R., Tracey, K.L., 1998. Determining geostrophic velocity shear profiles with inverted echo sounders. Journal of Geophysical Research 103 (C3), 5607–5622.

Hellerman, S., Rosenstein, M., 1983. Normal monthly wind stress over the world ocean with error estimates. Journal of Physical Oceanography 13, 1093–1104.

Hogg, N.G., 1992. On the transport of the Gulf Stream between Cape Hatteras and the Grand Banks. Deep-Sea Research 39, 1231–1246.

Johns, W.E., Shay, T.J., Bane, J.M., Watts, D.R., 1995. Gulf Stream structure, transport, and recirculation near 68°W. Journal of Geophysical Research 100 (1), 817–838.

Klein, B.K., Siedler, G., 1989. On the origin of the Azores Current. Journal of Geophysical Research 94, 6159–6168.

Krauss, W.M., 1986. The North Atlantic Current. Journal of Geophysical Research 91, 5061–5074.

Krauss, W.M., Fahrbach, E., Aitsam, A., Elken, J., Koske, P., 1987. The North Atlantic Current and its associated eddy field southeast of Flemish Cap. Deep-Sea Research 34, 1163–1185.

Lazier, J.R.N., 1994. Observations in the Northwest Corner of the North Atlantic Current. Journal of Physical Oceanography 24 (7), 1449–1463.

Lazier, J.R.N., Wright, D.G., 1993. Annual velocity variations in the Labrador Current. Journal of Physical Oceanography 23 (4), 659–678.

Lozier, M.S., Owens, W.B., Curry, R.G., 1995. The Climatology of the North Atlantic. Progress in Oceanography 36, 1–44.

Mann, C.R., 1967. The termination of the Gulf Stream and the beginning of the North Atlantic Current. Deep-Sea Research 14, 337–359.

McCartney, M.S., Talley, L.D., 1984. Warm-to-cold water conversion in the northern North Atlantic ocean. Journal of Physical Oceanography 14 (5), 922–935.

Meinen, C.S., Watts, D.R., 1998. Calibrating inverted echo sounders equipped with pressure sensors. Journal of Atmospheric and Oceanic Technology 15 (6), 1339–1345.

Meinen, C.S., Watts, D.R., 2000. Vertical structure and transport on a transect across the North Atlantic Current near 42°N: time series and mean. Journal of Geophysical Research 105 (C9), 21,869–21,891.

Meinen, C.S., Watts, D.R., Clarke, R.A., 2000. Absolutely referenced geostrophic velocity and transport on a section across the North Atlantic Current. Deep-Sea Research 47 (2), 309–322.

Mountain, D.G., Shuhy, J.L., 1980. Circulation near the Newfoundland Ridge. Journal of Marine Research 38, 205–213.

Peixoto, J.P., Oort, A.H., 1992. Physics of Climate. AIP Press, New York.

Pickart, R.S., Watts, D.R., 1990. Using the inverted echo sounder to measure vertical profiles of Gulf Stream temperature and geostrophic velocity. Journal of Atmospheric and Oceanic Technology 7, 146–156.

Qian, X., Watts, D.R., 1992. The SYNOP experiment: bottom pressure maps for the Central Array May 1988 to August 1990. Technical Report 3, Grad. School of Oceanography, Univ. of R.I., Narragansett, R.I.

Reiniger, R.F., Clarke, R.A., 1975. Circulation pattern in the newfoundland ridge area, 1972. In: Symposium on environmental conditions in the Newfoundland Grand Bank area in 1972 and their effect on fishery trends, Vol. 10. International Commission for the Northwest Atlantic Fisheries, Dartmouth, Canada, pp. 57–67.

Rice, J.A., 1988. Mathematical Statistics and Data Analysis.. Wadsworth, Belmont, CA.

Richardson, P.L., 1983. Eddy kinetic energy in the North Atlantic from surface drifters. Journal of Geophysical Research 88 (C7), 4355–4367.

Rossby, T., 1996. The North Atlantic Current and surrounding waters: at the crossroads. Reviews of Geophysics 34 (4), 463–481.

Schmitz Jr., W.J., 1981. Observations of eddies in the Newfoundland Basin. Deep-Sea Research 28A (11), 1417–1421.

Schmitz Jr., W.J., McCartney, M.S., 1993. On the North Atlantic circulation. Reviews of Geophysics 31, 29–49.

Sy, A., 1988. Investigation of large-scale circulation patterns in the central North Atlantic: the North Atlantic Current, the Azores Current, and the Mediterranean water plume in the area of the Mid-Atlantic Ridge. Deep-Sea Research 35, 383–413.

Sy, A., Schauer, U., Meincke, J., 1992. The North Atlantic Current and its associated hydrographic structure above and eastwards of the Mid-Atlantic Ridge. Deep-Sea Research 39 (5), 825–853.

Tomczak, M., Godfrey, J.S., 1994. Regional Oceanography: An Introduction. Pergamon, Oxford.

Watts, D.R., Qian, X., Tracey, K.L., 2001. On mapping abbysal current and pressure fields under the meandering Gulf Stream. Journal of Atmospheric and Oceanic Technology, in press.

Worthington, L.V., 1976. On the North Atlantic Circulation. The Johns Hopkins Oceanographic Studies, Vol. 6. The Johns Hopkins University Press, Baltimore, MD.